

**RECENT RESULTS ON THE MASS,  
GRAVITATIONAL FIELD  
AND MOMENTS OF INERTIA OF THE MOON\***

WILLIAM H. MICHAEL, Jr. and W. THOMAS BLACKSHEAR  
*NASA, Langley Research Center, Hampton, Va., U.S.A.*

(Received 25 September, 1971)

**Abstract.** Doppler tracking data from the Lunar Orbiter series of spacecraft have been used in a more complete analysis of the spherical harmonic coefficients of the lunar gravitational field through thirteenth degree and order. The value obtained for the mass of the Moon,  $GM = 4902.84 \text{ km}^3 \text{ s}^{-2}$ , is in good agreement with previous results and with results obtained by alternate procedures. Acceleration contour plots, derived from the gravitational coefficients, show correlations with surface features on the near side of the Moon, but are of questionable validity for the far side because of the lack of direct tracking data on the far side. Based on the most recent gravitational field data, the current estimate for the polar moment of inertia of the Moon is  $C/Ma^2 = 0.4019_{-0.002}^{+0.004}$ . This value indicates that the interior of the Moon can be homogeneous, but some results presented strongly suggest that the Moon is differentiated, with an excess of mass in the direction toward the Earth.

### 1. Introduction

A more complete analysis of Doppler tracking data from the Lunar Orbiter series of artificial lunar satellites has been performed in an effort to provide an improved estimate of the gravitational field of the Moon. The objective of such an analysis is to determine the coefficients  $C_{n,m}$  and  $S_{n,m}$  of a finite number of terms in the infinite series expansion of the lunar gravitational potential function as expressed in spherical harmonics of the form

$$U = \frac{GM}{r} \left[ C_{0,0} + \sum_{n=2}^{\infty} \sum_{m=0}^n \left( \frac{a}{r} \right)^n P_{n,m} \sin \phi (C_{n,m} \cos m\lambda + S_{n,m} \sin m\lambda) \right].$$

In this expression,  $GM$  is the product of the gravitational constant and the mass of the Moon,  $a$  is the mean radius of the Moon (taken here as 1738.09 km),  $r$  is the radial distance from the lunar center of mass,  $P_{n,m}$  are the associated Legendre polynomials of degree  $n$  and order  $m$ ,  $\phi$  is selenographic latitude, and  $\lambda$  is selenographic longitude. Previous results in a series of lunar gravitational field analyses performed at the Langley Research Center have been summarized by Michael *et al.* (1970). These authors presented a solution for gravitational coefficients through thirteenth degree and order, based on 12600 Doppler observations. The results given here, also through thirteenth degree and order in the coefficients, are based on considerable additional data comprising some 20000 Doppler observations.

\* Paper presented at the NATO Advanced Study Institute on Lunar Studies, Patras, Greece, September, 1971.

There are three major obstacles which cause limitations in efforts to determine a precise definition of the lunar gravitational field. The first is that direct line-of-sight observation of a lunar orbiting spacecraft is interrupted as it moves behind the Moon, so that direct data coverage of the lunar far side is not obtainable from Earth-based tracking stations. The second is that the variety of orbital parameters covered by lunar satellites established thus far is still relatively limited. The third is that the Moon is a wonderfully complicated gravitational object, with many localized gravitational anomalies near its surface and perhaps in its interior, and these anomalies are difficult to represent in a finite mathematical formulation.

There is very little that can be done about the third obstacle, except perhaps to enjoy the challenge. The first two, however, can be alleviated by establishing additional lunar satellites and by incorporating new data gathering techniques to provide far side data, such as satellite-to-satellite tracking and far side beacons or retroreflectors. Indeed, some of the data obtained in the Apollo 15 mission, including tracking data from the subsatellite left in lunar orbit, and the laser altimeter data, will contribute to the gravitational field analysis problem.

Because of the complexity involved in determining the characteristics of the lunar gravitational field, a number of approaches have been attempted other than the one described here. Among the more interesting are the analysis by Muller and Sjogren (1968), and subsequent analyses, which have directly determined spacecraft accelerations and correlations of these with lunar surface features, thus describing local gravitational anomalies in considerable detail. Several other approaches to the general problem of lunar gravitational field determination are summarized by Michael *et al.* (1970).

## 2. Method of Analysis and Data Coverage

The procedure used for the gravitational field determination results presented here is a weighted-least-squares, differential correction process with numerical integration of the spacecraft equations of motion, and the associated variational equations. The basic observable is the number of cycles in the Doppler frequency shift of a radio signal sent from an Earth-station to the spacecraft and received back at an Earth-station, averaged over a one-minute counting time. Other quantities required in the differential correction process are the calculated value of the observable and the partial derivatives of the observable with respect to the set of parameters to be corrected, evaluated at each of the times at which the Doppler frequency shift is measured. The calculated values of the observable are derived from the numerical integration of the (Cowell-type) equations of motion of the spacecraft, using a twelfth-order predictor-corrector technique, starting with initial estimates of the spacecraft state at the initial epoch of a series of orbits. The partial derivatives, of the observable with respect to the set of parameters to be corrected, are derived from a similar numerical integration of the variational equations which relate the change in the observable to changes in the initial estimates of the parameters to be corrected. Using the quantities thus defined the differential correction process yields, with

considerable manipulation on a large-scale digital computer, a weighted-least-squares estimate of the corrections to be applied to the initial values of the set of parameters in the solution. Since this process is a linearized approximation to a non-linear problem, the solution must be iterated until the solution converges and the changes become acceptably small.

TABLE I  
Orbital geometry and tracking data

	Lunar Orbiter					
	1	2	3a	3b	4	5
Semimajor axis, km	2670	2702	2688	1968	3751	2832
Eccentricity	0.327	0.341	0.332	0.062	0.516	0.317
Inclination, <sup>a</sup> deg	12	18	21	21	84	85
Period, min	206	210	208	130	344	225
Data arcs	2	3	3	5	2	8
Total length of arcs, days	9.7	8.5	15.9	17.1	8.6	19.9
Observations	2076	2662	2502	3322	3739	5847

<sup>a</sup> inclination to lunar equator.

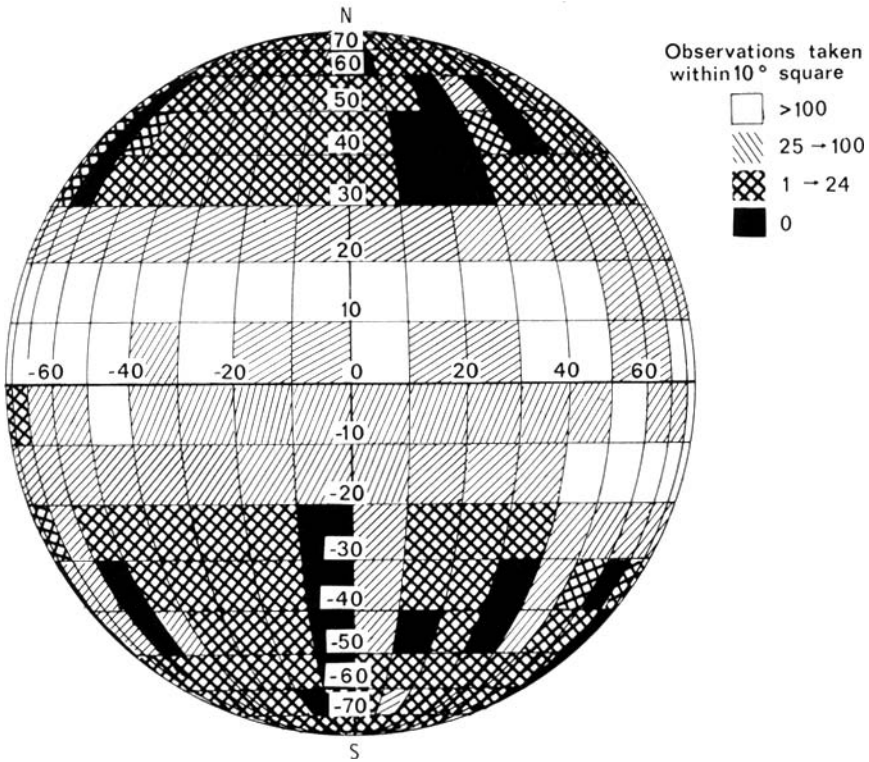


Fig. 1a. Lunar near side – total data coverage.

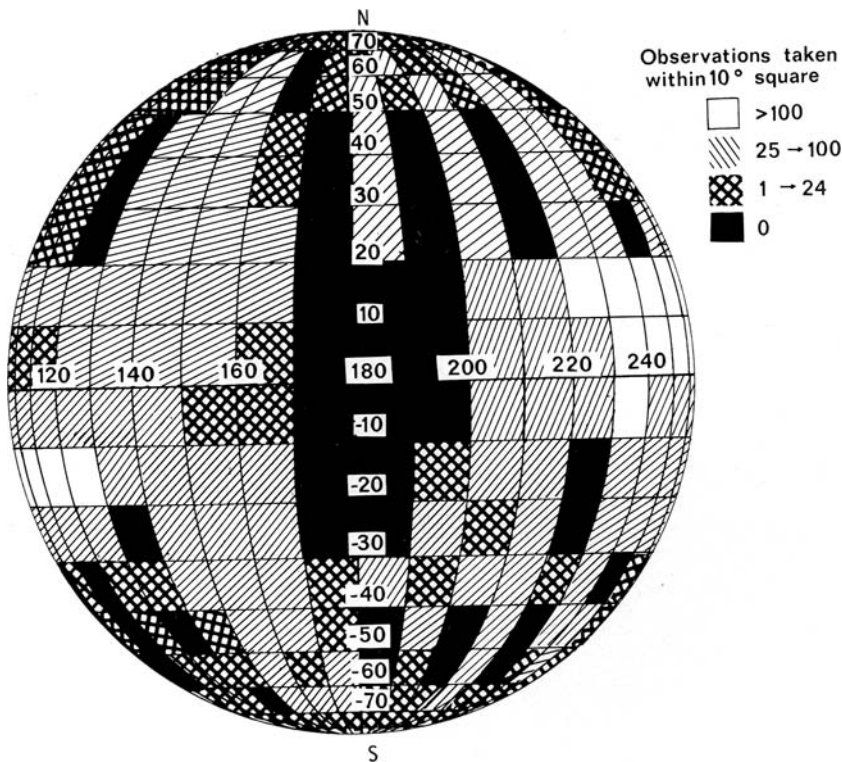


Fig. 1b. Lunar far side – concluded.

The orbital geometry, data arcs (data representing a continuous spacecraft trajectory), number of data points (Doppler shift observables), and total length of arcs used in this current analysis are shown in Table I. Six separate orbital geometries from all five of the Lunar Orbiter missions, 20, 148 coherent two-way Doppler observations, and approximately 80 days of tracking coverage have been included. The set of parameters in this solution contains (with six state parameters for each of the 23 different arcs and 193 gravitational coefficients) 331 quantities to be differentially corrected in the iteration process.

It is of interest to illustrate how the data coverage of Table I is actually distributed over the surface of the Moon. This is shown in Figure 1, for the total data, independent of spacecraft altitude. Figure 2 shows the observations taken on the near side of the Moon when the spacecraft were below 200 km altitude; there is essentially no coverage on the far side at altitudes below 200 km altitude. As indicated, the best coverage is between  $-20^\circ$  and  $+30^\circ$  selenographic latitude on the front side, with considerably decreased coverage in the polar regions and on the far side. As a result of radial attenuation of gravitational effects, the data in the high latitude and far side regions are clearly less sensitive to localized gravitational anomalies than the mid-latitude region on the front side.

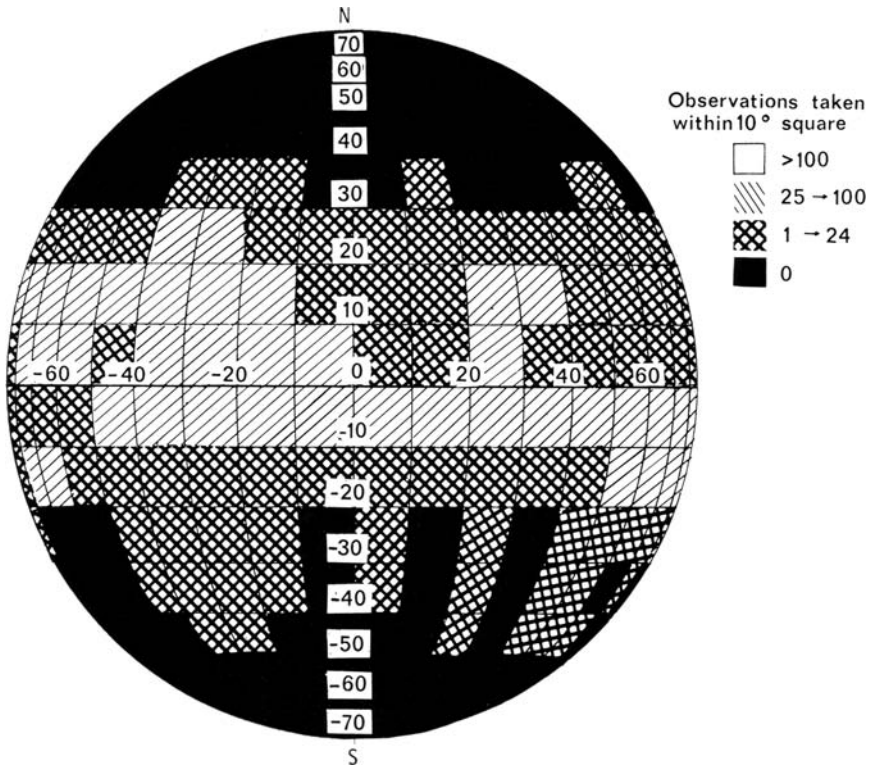


Fig. 2. Lunar near side - observations taken when the spacecraft was below 200 km altitude.

Although areas are shown in Figures 1 and 2 in which no direct observations were made, these regions are indirectly represented in that the net effect of the gravitational forces in these regions is reflected in the continuous spacecraft orbits and hence in the data. The same comment applies in a more restricted manner to the lunar far side, where at least the integrated effects of the gravitational forces are represented in the directly-observed data. However, the lack of complete global coverage of direct data and/or low altitude data remains an important limitation in the effort to provide a rigorous mathematical description of the lunar gravitational field.

### 3. Results for the Mass and Gravitational Field of the Moon

The results of the present analysis of the lunar gravitational field harmonic coefficients through thirteenth degree and order are presented in Table II. The result given for  $C_{0,0}$  implies a value of  $4902.84 \text{ km}^3 \text{ s}^{-2}$  for  $GM$ , as compared with  $4902.86 \text{ km}^3 \text{ s}^{-2}$  for the previous thirteenth degree solution; and is in good agreement with the value of  $4902.75 \text{ km}^3 \text{ s}^{-2}$  obtained from a combination of analyses from deep space probes using a different technique. A comparison of some parameters from the present and

TABLE II  
Coefficients of the thirteenth degree and order solution  
for lunar gravitational field

$n$	$m$	$C_{n,m}$	$S_{n,m}$
0	0	1.00005388274	
2	0	$-2.0378761820 \times 10^{-4}$	0
	1	$1.1051542512 \times 10^{-5}$	$1.3006148287 \times 10^{-5}$
	2	$2.4845211490 \times 10^{-5}$	$-1.0442661244 \times 10^{-8}$
3	0	$2.8439912986 \times 10^{-5}$	0
	1	$2.4152698939 \times 10^{-5}$	$2.0805931299 \times 10^{-5}$
	2	$7.6322652451 \times 10^{-6}$	$2.2710804784 \times 10^{-6}$
	3	$1.4111967268 \times 10^{-6}$	$-3.1126414977 \times 10^{-7}$
4	0	$3.4688330254 \times 10^{-5}$	0
	1	$-1.9891933273 \times 10^{-5}$	$-8.5100449545 \times 10^{-6}$
	2	$-2.5443614074 \times 10^{-6}$	$-4.1656170604 \times 10^{-6}$
	3	$-5.6321036284 \times 10^{-7}$	$-2.7682641529 \times 10^{-7}$
	4	$-5.3981736976 \times 10^{-8}$	$1.1411256460 \times 10^{-7}$
5	0	$-2.6623483022 \times 10^{-5}$	0
	1	$-7.4939720619 \times 10^{-6}$	$-9.2535826576 \times 10^{-6}$
	2	$3.4603506756 \times 10^{-7}$	$3.8762399793 \times 10^{-7}$
	3	$4.0040015934 \times 10^{-7}$	$8.8773988822 \times 10^{-7}$
	4	$9.3924925003 \times 10^{-8}$	$-1.4794482739 \times 10^{-7}$
	5	$1.8771823966 \times 10^{-8}$	$-2.1001366939 \times 10^{-8}$
6	0	$4.9673195626 \times 10^{-5}$	0
	1	$-1.8543318257 \times 10^{-5}$	$-9.5673010658 \times 10^{-6}$
	2	$-5.5091031933 \times 10^{-7}$	$1.8138036159 \times 10^{-7}$
	3	$1.1678358571 \times 10^{-7}$	$-1.1841174024 \times 10^{-7}$
	4	$-3.3956313198 \times 10^{-8}$	$-9.7021389127 \times 10^{-8}$
	5	$-9.6847691920 \times 10^{-9}$	$8.1237744599 \times 10^{-9}$
	6	$-4.0790023093 \times 10^{-9}$	$2.9739566973 \times 10^{-9}$
7	0	$-7.2781850970 \times 10^{-5}$	0
	1	$4.1810263527 \times 10^{-6}$	$-2.8408094790 \times 10^{-5}$
	2	$-8.3378247684 \times 10^{-7}$	$-7.4166186129 \times 10^{-7}$
	3	$-1.2737535124 \times 10^{-7}$	$-1.7509754956 \times 10^{-7}$
	4	$-4.1682647653 \times 10^{-8}$	$-2.5407115475 \times 10^{-9}$
	5	$1.8658206027 \times 10^{-9}$	$1.0910340047 \times 10^{-8}$
	6	$4.6261404574 \times 10^{-10}$	$-7.1046094393 \times 10^{-10}$
	7	$3.4334519153 \times 10^{-10}$	$-1.2401781124 \times 10^{-10}$
8	0	$-1.7411742627 \times 10^{-5}$	0
	1	$1.3701858067 \times 10^{-5}$	$3.6716642133 \times 10^{-6}$
	2	$4.0795796661 \times 10^{-7}$	$9.1385019071 \times 10^{-7}$
	3	$9.3910161964 \times 10^{-9}$	$-1.9359154697 \times 10^{-7}$
	4	$-6.4523074373 \times 10^{-9}$	$2.5059489581 \times 10^{-8}$
	5	$4.5024517927 \times 10^{-9}$	$-9.1723952804 \times 10^{-10}$
	6	$3.6434678341 \times 10^{-10}$	$-1.0430917747 \times 10^{-9}$
	7	$-1.4858612477 \times 10^{-11}$	$2.1525564980 \times 10^{-11}$
	8	$-3.6012675699 \times 10^{-11}$	$1.1935027479 \times 10^{-11}$

Table II (Continued)

$n$	$m$	$C_{n,m}$	$S_{n,m}$
9	0	$-6.5011326253 \times 10^{-5}$	0
	1	$5.3770904532 \times 10^{-7}$	$-5.2273480368 \times 10^{-6}$
	2	$-4.4206541496 \times 10^{-7}$	$-3.1727246486 \times 10^{-7}$
	3	$-1.2910912315 \times 10^{-7}$	$-5.4900413900 \times 10^{-8}$
	4	$-8.3591988861 \times 10^{-9}$	$2.1240873880 \times 10^{-8}$
	5	$8.7259392768 \times 10^{-10}$	$-2.5124288158 \times 10^{-9}$
	6	$-5.1505398116 \times 10^{-10}$	$1.2516041989 \times 10^{-10}$
	7	$-8.0690242529 \times 10^{-11}$	$8.0754026764 \times 10^{-11}$
	8	$-1.2649479578 \times 10^{-12}$	$2.6681227345 \times 10^{-11}$
	9	$1.7805101055 \times 10^{-12}$	$-5.4376209997 \times 10^{-13}$
10	0	$-1.9534030711 \times 10^{-5}$	0
	1	$3.5640472538 \times 10^{-5}$	$4.51233094077 \times 10^{-7}$
	2	$4.9196310871 \times 10^{-9}$	$5.7169685637 \times 10^{-7}$
	3	$-2.2358784038 \times 10^{-9}$	$-3.6437585575 \times 10^{-8}$
	4	$3.9141653049 \times 10^{-9}$	$1.1269567323 \times 10^{-8}$
	5	$3.8087666364 \times 10^{-10}$	$-2.1308938653 \times 10^{-9}$
	6	$-4.6255135189 \times 10^{-11}$	$1.5652458548 \times 10^{-10}$
	7	$2.7614962503 \times 10^{-11}$	$-1.5540376682 \times 10^{-11}$
	8	$5.4896743830 \times 10^{-12}$	$-4.0505042040 \times 10^{-12}$
	9	$9.2407535252 \times 10^{-14}$	$-3.6136326596 \times 10^{-13}$
	10	$-7.5223488683 \times 10^{-14}$	$3.3135927064 \times 10^{-14}$
11	0	$5.1037452530 \times 10^{-5}$	0
	1	$-7.7291781814 \times 10^{-6}$	$2.8479446434 \times 10^{-5}$
	2	$-3.2273658086 \times 10^{-7}$	$7.2497774428 \times 10^{-7}$
	3	$2.3360853505 \times 10^{-8}$	$5.5966682329 \times 10^{-8}$
	4	$1.0287849331 \times 10^{-9}$	$1.3205804852 \times 10^{-8}$
	5	$-3.1877004821 \times 10^{-10}$	$-8.8603014695 \times 10^{-10}$
	6	$6.2535668259 \times 10^{-11}$	$1.2557575513 \times 10^{-10}$
	7	$-1.3948668302 \times 10^{-12}$	$-1.6191981587 \times 10^{-11}$
	8	$-9.6800165098 \times 10^{-13}$	$2.8512390282 \times 10^{-13}$
	9	$-2.8524797963 \times 10^{-13}$	$2.5679558039 \times 10^{-13}$
	10	$-1.4876779292 \times 10^{-14}$	$2.0466569257 \times 10^{-14}$
	11	$7.2963987090 \times 10^{-16}$	$-1.1859856626 \times 10^{-15}$
12	0	$9.7617164640 \times 10^{-6}$	0
	1	$1.2778274406 \times 10^{-5}$	$1.4438415728 \times 10^{-6}$
	2	$-1.5405505424 \times 10^{-7}$	$5.3551638732 \times 10^{-7}$
	3	$5.4002051640 \times 10^{-9}$	$8.7868585746 \times 10^{-9}$
	4	$4.0078293255 \times 10^{-9}$	$1.2737288951 \times 10^{-9}$
	5	$9.5030429269 \times 10^{-11}$	$-4.8376477908 \times 10^{-10}$
	6	$1.7093579633 \times 10^{-11}$	$6.0134093338 \times 10^{-12}$
	7	$-7.2263198820 \times 10^{-13}$	$-5.5677059494 \times 10^{-12}$
	8	$1.2421199266 \times 10^{-13}$	$9.7510387449 \times 10^{-13}$
	9	$-3.7285776082 \times 10^{-14}$	$-2.4368928834 \times 10^{-14}$
	10	$9.9312843321 \times 10^{-15}$	$-1.0618795919 \times 10^{-14}$
	11	$5.2033681565 \times 10^{-16}$	$-4.2870250967 \times 10^{-16}$
	12	$-2.3855459682 \times 10^{-18}$	$4.5543340194 \times 10^{-18}$
13	0	$7.5782274244 \times 10^{-6}$	0
	1	$-5.7637379713 \times 10^{-6}$	$2.3610613996 \times 10^{-5}$

Table II (Continued)

<i>n</i>	<i>m</i>	<i>C<sub>n,m</sub></i>	<i>S<sub>n,m</sub></i>
13	2	$-1.5991666946 \times 10^{-7}$	$3.4297075982 \times 10^{-7}$
	3	$2.7190638195 \times 10^{-8}$	$9.6757608497 \times 10^{-9}$
	4	$7.6732684554 \times 10^{-10}$	$3.0028913747 \times 10^{-9}$
	5	$-2.1117612255 \times 10^{-10}$	$-1.1279989530 \times 10^{-10}$
	6	$1.8106651096 \times 10^{-11}$	$1.9737118563 \times 10^{-11}$
	7	$-1.6221201052 \times 10^{-12}$	$-1.1582995210 \times 10^{-12}$
	8	$-8.7167027819 \times 10^{-14}$	$8.6768075576 \times 10^{-14}$
	9	$1.0705140705 \times 10^{-14}$	$-2.7869365761 \times 10^{-14}$
	10	$-7.5223488683 \times 10^{-14}$	$3.3135927064 \times 10^{-14}$
	11	$-2.8387572286 \times 10^{-16}$	$2.0316367811 \times 10^{-16}$
	12	$-9.0639928622 \times 10^{-18}$	$-1.2565366439 \times 10^{-17}$
	13	$1.1380844737 \times 10^{-18}$	$-2.6006569878 \times 10^{-19}$

TABLE III

Comparison of gravitational parameters from thirteenth degree and order solution

Solution	1969	1971
Number of observations	12600	20148
<i>GM</i> , km <sup>3</sup> s <sup>-2</sup>	4902.86	4902.84
<i>C<sub>2,0</sub></i>	$-2.071 \times 10^{-4}$	$-2.038 \times 10^{-4}$
<i>C<sub>2,2</sub></i>	$2.242 \times 10^{-5}$	$2.485 \times 10^{-5}$
<i>C<sub>2,1</sub></i>	$-0.044 \times 10^{-5}$	$1.105 \times 10^{-5}$
<i>S<sub>2,1</sub></i>	$-0.457 \times 10^{-5}$	$1.301 \times 10^{-5}$
<i>S<sub>2,2</sub></i>	$0.021 \times 10^{-5}$	$-0.001 \times 10^{-5}$

previous solutions, which are of particular interest for subsequent discussion, is given in Table III.

With the exception of some of the low-degree coefficients in Table II, a term-by-term comparison of coefficients from various solutions is not considered particularly meaningful, mainly because of high correlations between a number of the various coefficients. Thus general comparisons should be made only on the basis of the complete set of coefficients for a solution.

The overall characteristics of the present solution are best represented by contour maps of the radial component of gravitational acceleration, as shown in Figure 3. The contours are in terms of milligals ( $10^{-3}$  cm s<sup>-2</sup>) and represent the deviations in the radial acceleration from that of a spherically symmetric field, for which  $GM=4902.84$  km<sup>3</sup> s<sup>-2</sup>, plotted for an altitude of 100 km above the mean lunar surface. The three large northern hemisphere positive anomalies occurring below 40° latitude in Figure 3a correspond closely to the lunar maria Imbrium, Serenitatis, and Crisium, as well as areas of high data coverage. The relatively large positive and negative anomalies



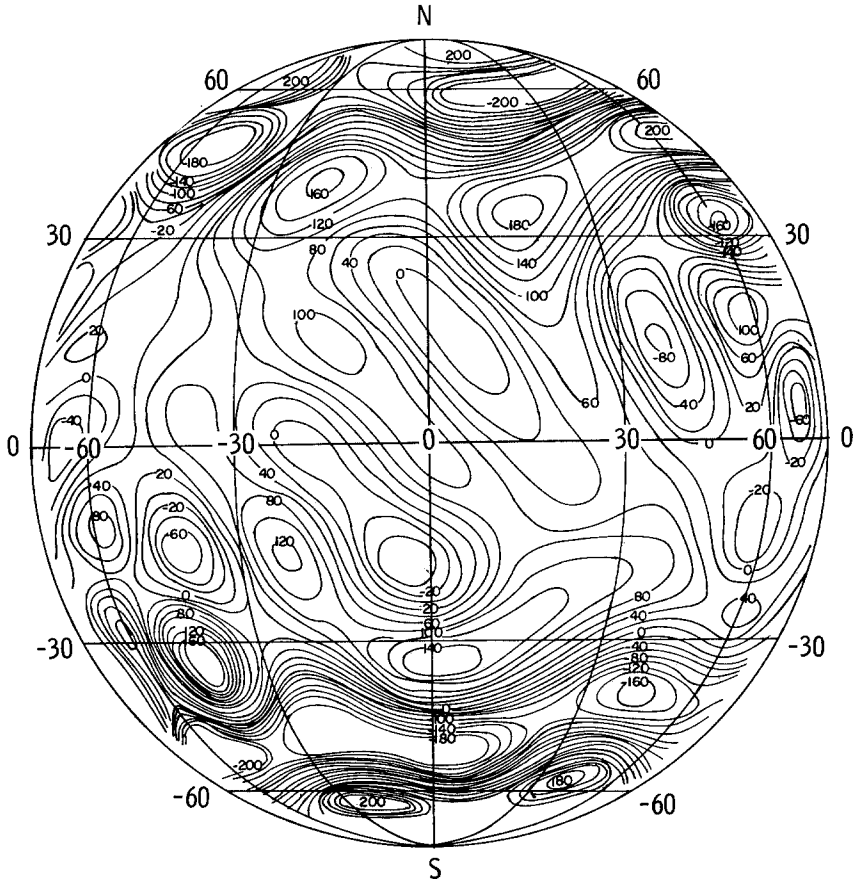


Fig. 3a. Lunar near side - estimate of variations in gravitational acceleration (milligals).

in the polar regions on the front side and throughout the far side exhibit a strong correlation with the regions of less dense data coverage of Figures 1 and 2. It is thus considered that the gravitational field representation in the central latitude region on the front side of the Moon is much more valid than that in other regions.

One advantage of a general representation of the gravitational field is that the field can be evaluated at any desired altitude, and the variation with altitude can be used for analysis of gravitational anomalies. A rough estimate of the density distribution of the Imbrium and Serenitatis gravitational anomalies can be obtained by assuming a point-source model for the mass producing the anomaly. The gravitational field of point sources for these regions was expanded in spherical harmonics to the same degree and order as the current estimate of the gravitational field. By the method of least squares, this expansion was then fitted to the gravitational field estimate over regions around the anomaly varying from 50 to 150 km in altitude and  $10^\circ$  in selenocentric angle from the axis of the anomaly. The resulting solutions for the sizes and

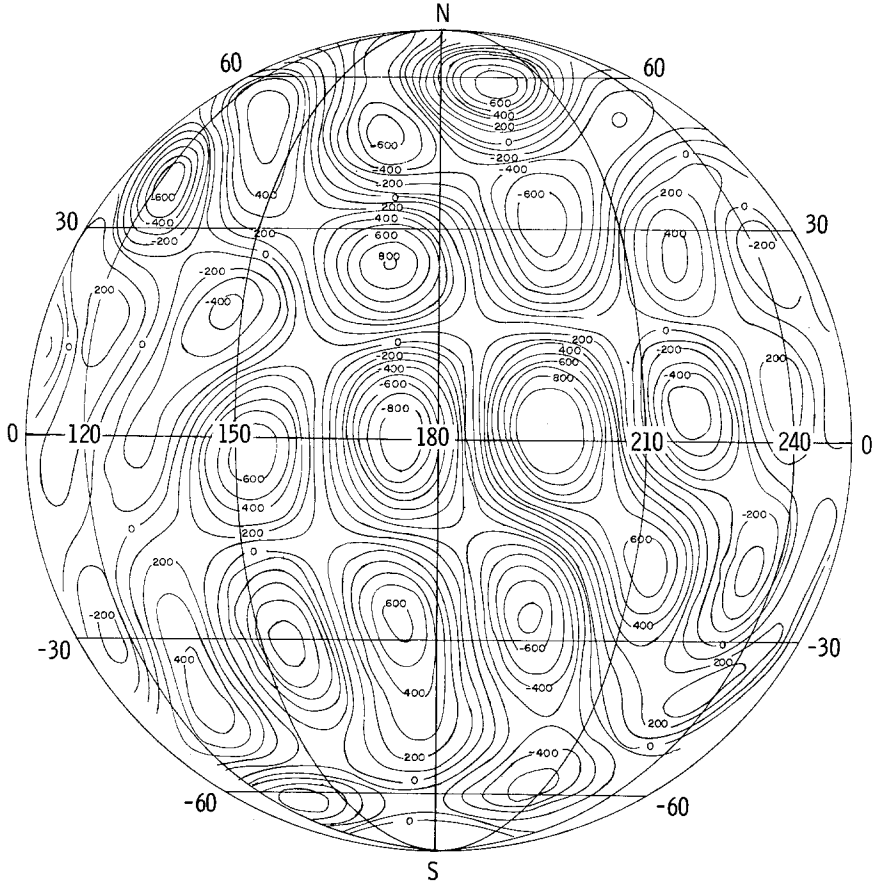


Fig. 3b. Lunar far side – concluded.

TABLE IV  
Point source approximations

	Mass/Lunar mass	Radius, km	Latitude, deg	Longitude, deg
Imbrium	$7.68 \times 10^{-5}$	1450	33.8	16.3
Serenitatis	$4.17 \times 10^{-5}$	1546	29.0	-20.5

locations of the point masses are given in Table IV, indicating large mass concentrations at the depths of 200 to 300 km below the surface. Figure 4 shows the degree of agreement between the point source solution and the spherical harmonic estimate of the Serenitatis anomaly. This exercise illustrates the type of investigation that can be conducted with a more refined gravitational field estimate and more elaborate source models.

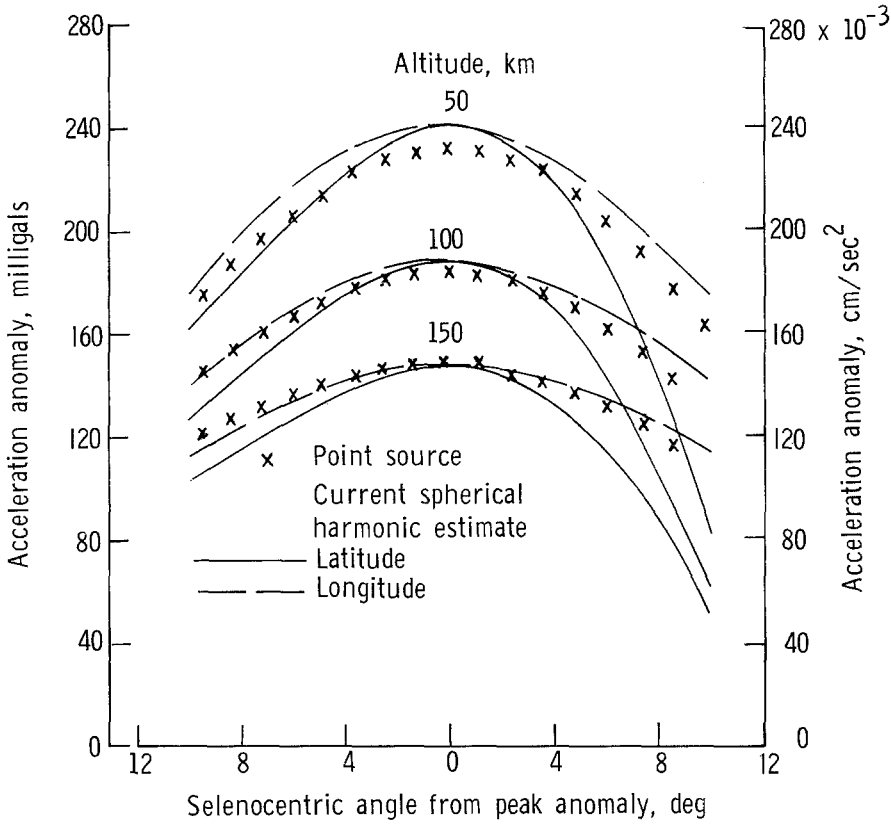


Fig. 4. Point source and spherical harmonic estimates of the Serenitatis gravitational anomaly as function of latitude and longitude. 1 milligal =  $1 \times 10^{-8} \text{ cm s}^{-2}$ .

#### 4. Moments of Inertia of the Moon

The moments of inertia of the Moon are of particular interest in studies of the geophysics of the Moon, as an indication of the overall distribution of mass and density in the lunar interior. Moments of inertia cannot be derived solely on the basis of the lunar gravitational field coefficients. Other independent information, particularly that from studies of the physical librations of the Moon, can be used in conjunction with the gravitational field data to provide the moment of inertia estimates.

The second-degree coefficients in the lunar gravitational potential function can be related to moments and products of inertia by the relations

$$C_{2,0} = \frac{1}{Ma^2} \left[ \frac{A+B}{2} - C \right]; \quad C_{2,2} = \frac{1}{4Ma^2} (B-A);$$

$$C_{2,1} = \frac{E}{Ma^2}; \quad S_{2,1} = \frac{D}{Ma^2}; \quad S_{2,2} = \frac{F}{2Ma^2}.$$

In these expressions,  $A$  is the moment of inertia about an axis in the lunar equatorial plane directed along the mean Moon-Earth line ( $x$ -axis),  $C$  is the moment of inertia about the axis of rotation of the Moon ( $z$ -axis), and  $B$  is that about the axis in the equatorial plane perpendicular to  $x$  and  $z$  ( $y$ -axis).  $D$ ,  $E$ , and  $F$  are the products of inertia related to the  $yz$ ,  $xz$ , and  $xy$  axes, respectively. Finally,  $M$  is the mass of the Moon, and  $a$  is the mean radius of the Moon taken here as the same value (1738.09 km) used in the gravitational field analysis.

As previously indicated, the five relations given above are not sufficient to determine the six moments and products of inertia required for the inertia tensor from which the principal moments of inertia are calculated. Several options are available, from studies of the physical librations of the Moon and the inclination of the lunar equator to the ecliptic, for a sixth relation. Koziel (1967) has reduced several series of heliometer observations, of the distance from the crater Mösting A to the limb of the Moon, to obtain results for the quantities

$$\beta = \frac{C - A}{B} \quad \text{and} \quad f = \frac{\alpha}{\beta} = \frac{(C - B) B}{(C - A) A}.$$

Jeffreys (1961) has developed a theory for the physical librations of the Moon and has presented results of calculations for  $\beta$ , based on determinations of the inclination of the lunar equator to the ecliptic by various authors, and results for  $\gamma$ , where

$$\gamma = \frac{B - C}{C}$$

derived from the libration in longitude. Cook (1970) has presented a summary of the various data sources for libration constants and has obtained least squares solutions for the polar moment of inertia and libration constants using combined sets of data from a number of sources. Even more recently, Jeffreys (1971) has considered the effects of elasticity of the Moon on the libration constants and has derived revised values for  $\beta$  and  $\gamma$  including these effects.

It seems that the determinations of  $\beta$  provide the most reliable of the libration constant estimates, whereas the values of  $\gamma$  and  $f$  (which can be related through the approximate expression  $f \cong 1 - \gamma/\beta$ ) differ significantly among some of the determinations noted above. Koziel (1967) and Jeffreys (1971) both give the value,  $\beta = 6.29 \times 10^{-4}$ . Adopting this value and using it in combination with the coefficients in Table II, the results for the principal moments of inertia of the Moon are

$$\frac{C}{Ma^2} = 0.403141 \quad \frac{B}{Ma^2} = 0.402985 \quad \frac{A}{Ma^2} = 0.402886$$

The corresponding values from the 1969 solution, with  $\beta$  as defined by Koziel (1967) are 0.400663, 0.400500, and 0.400410, respectively. The principal moments of inertia do not differ from the moments of inertia about the  $x$ ,  $y$ , and  $z$  (body) axes to the number of places given.

The 1969 and 1971 results for  $C/Ma^2$  are considered to be of approximately equal validity, which suggests that an average of the two results,  $C/Ma^2 = 0.4019$ , be used as the current best estimate. The corresponding average value for  $f$  is 0.631, which is in very good agreement with the value of  $f = 0.633$  derived by Koziel (1967). Cook (1970) presents results for which he finds a value of  $\beta = 6.25 \times 10^{-4}$  more consistent with other data than the value  $\beta = 6.29 \times 10^{-4}$  used in this analysis. Using  $\beta = 6.25 \times 10^{-4}$  yields  $C/Ma^2$  of 0.4032 and 0.4057, respectively, for the 1969 and 1971 gravitational coefficients, which gives some indication of the variation of the results. With the above considerations, the current estimate of the polar moment of inertia of the Moon is

$$\frac{C}{Ma^2} = 0.4019_{-0.002}^{+0.004}$$

where the uncertainties are somewhat arbitrary.

It should be noted that Cook (1970) derives values for  $C/Ma^2$  ranging from 0.3937 to 0.3978 in his paper, but with a new (1970) value for  $\gamma$  from Sir Harold Jeffreys, Cook obtains  $C/Ma^2 = 0.4032$  in a solution with the least residuals, in a note added in proof.

### 5. Implications of Moment of Inertia Results

The moment of inertia of a solid homogeneous sphere is 0.4, and  $C/Ma^2$  for the Earth is about 0.33, indicating a considerable increase in density toward the center of the Earth. The estimate of  $C/Ma^2$  of 0.4019 for the Moon implies a slight overall decrease of density toward its center, differentiation of the interior of the Moon with some concentration of higher than mean density material near the surface, or some other unusual density distribution.

A chemically homogeneous moon could result in a moment of inertia value greater than 0.4. Levin (1966) presents models for density variations with depth in which he indicates that the increase of density toward the center of the Moon due to gravitational (pressure) effects and the decrease due to thermal expansion effects are almost equal. Using his smaller compressibility and larger thermal expansion coefficient effects, and scaling his density variations to obtain the proper value for the mean density of the moon ( $3.34 \text{ gm cm}^{-3}$ ), one can obtain values for  $C/Ma^2$  in the range of 0.401 to 0.402. Urey and MacDonald (1971) have used thermal expansion and compressibility coefficients for olivine in calculations which yield  $C/Ma^2 = 0.4004$ . Nakamura and Latham (1969) have considered 11 chemically homogeneous models for the Moon, for which the average value obtained for  $C/Ma^2$  was  $0.401 \pm 0.001$ . These results, compared with the moment of inertia value given herein, indicate that the Moon can be a chemically homogeneous body.

Within the uncertainties given for  $C/Ma^2$ , however, a large variety of lunar interior characteristics can be derived. For example, from calculations using simple two-layer models, the moment of inertia can be reduced by about 0.002 with a 250 km radius core of density  $8.0 \text{ gm cm}^{-3}$  with outer-density of  $3.32 \text{ gm cm}^{-3}$ . It can also be reduced by 0.002 with a 200 km thick crust of density  $3.27 \text{ gm cm}^{-3}$  with interior

density of  $3.38 \text{ gm cm}^{-3}$ . It can be increased by about 0.004 with a 190 km deep crust of density  $3.5 \text{ gm/cm}^{-3}$  with inner density of  $3.27 \text{ gm cm}^{-3}$ , etc.

Another quite interesting possibility is suggested from consideration of an apparent difference between the center of mass and center of figure of the Moon. Michael (1969) and Compton and Wells (1969) have pointed out, from limited lunar radii determinations, that the center of mass of the Moon may be about 2 km closer to the Earth than the center of figure of the Moon. Although details are not available at this writing, the Apollo 15 laser altimeter results apparently also indicate such an asymmetry, of perhaps larger magnitude. With the assumption of a 2-km difference between the center of figure and center of mass of the Moon, two-layer models have been generated which result in the given asymmetry, with a higher than mean density layer on the near side of the Moon, between  $\pm 60^\circ$  selenographic latitude and  $\pm 90^\circ$  selenographic longitude. The results are given in Table V. For slab thicknesses up to about 50 km, the resulting values of  $C/Ma^2$  are 0.4013, which is in good agreement with the 0.4019 value given here. This result strongly suggests that the Moon is somewhat differentiated, with an excess of mass in the direction toward the Earth.

TABLE V  
Moment of inertia due to a higher density Earth-side slab

Slab density, $\text{g cm}^{-3}$	Density elsewhere, $\text{g cm}^{-3}$	Slab depth, km	$C/Ma^2$
4.288	3.334	10	0.40128
3.815	3.334	20	0.40127
3.658	3.334	30	0.40126
3.579	3.334	40	0.40126
3.532	3.334	50	0.40125
3.356	3.333	1000	0.40075

In summary, the current results for the moment of inertia of the Moon indicate that the interior of the Moon can be homogeneous, but some of the results presented here strongly suggest that the moon is differentiated, with an excess of mass in the direction toward the earth.

## 6. Concluding Remarks

Further progress toward a precise definition of the lunar gravitational field, and the application of the results to problems in lunar geophysics, depends strongly on the obtaining of new data. Data from Apollo 15 and later Apollo missions, particularly the laser altimeter data and the tracking data from the subsatellite left in orbit around the Moon, will contribute to the analyses. Nevertheless, there is a definite need for alternate data-gathering procedures, other than direct Earth-based tracking, to provide geodesy-related data on the far side of the Moon. Some of the possibilities have been mentioned in a previous section of this paper. In consideration of the resources required for developing and establishing such techniques, advanced lunar exploration projects are possible candidates for implementation through international cooperation by interested nations.

### References

- Compton, H. R. and Wells, W. R.: 1969, 'Determination of Lunar Equatorial Radius Using Image-Motion Compensation Sensor Data from Lunar Orbiter I', NASA Technical Note D-5231.
- Cook, A. H.: 1970, *Monthly Notices Roy. Astron. Soc.* **150**, 187-194.
- Jeffreys, H.: 1961, *Monthly Notices Roy. Astron. Soc.* **122**, 421-432.
- Jeffreys, H.: 1971, Personal communication.
- Koziel, K.: 1967, *Icarus* **7**, 1-28.
- Levin, B. J.: 1966, 'The Structure of the Moon', Proc. California Institute of Technology - Jet Propulsion Laboratory Lunar and Planetary Conferences, California Institute of Technology, Pasadena, California.
- Michael, W. H. Jr.: 1969, 'The Figure of the Moon'. In Analysis of Apollo 8 Photography and Visual Observations, NASA SP-201.
- Michael, W. H. Jr., Blackshear, W. T., and Gapcynski, J. P.: 1970, in Bruno Morando (ed.), *Results on the Mass and Gravitational Field of the Moon as Determined from Dynamics of Lunar Satellites (1969)*, Springer-Verlag, pp. 42-56.
- Muller, P. M. and Sjogren, W. L.: 1968, *Science* **161**, 680-684.
- Nakamura, Y. and Latham, G. V.: 1969, *J. Geophys. Res.* **74**, 3771-3780.
- Urey, H. C. and Mac-Donald, G. J. F.: 1971, in Zdeněk Kopal (ed.), *Origin and History of the Moon. Physics and Astronomy of the Moon*, Second Edition, Academic Press, pp. 213-289.